



Dynamics of Land Use and Land Cover Change in the South Talihya Watershed North Kivu, Eastern Democratic Republic of Congo

Musubao Kapiri Moïse¹, Pierre Ozer², Mulondi Kayitoghera Gloire¹, Ahadi Mahamba Jonathan¹, Uzimati Djurua Isaac³, Musongora Kambale Muyisa⁴, Kahambu Matimbya Hintou¹, Muhindo Sahani Walere⁴

¹Laboratory of Ecology, Geomorphology and Geomatics, Catholic University of the Graben, Democratic Republic of Congo

²Department of Environmental Sciences and Management, University of Liège, Belgium

³Urban Planning Section, Institute of Buildings and Public Works, Democratic Republic of Congo

⁴Department of Water and Forests Resource Management, Catholic University of the Graben, Democratic Republic of Congo

Corresponding Author: Musubao Kapiri Moïse; Email: musubaokapiri@gmail.com

ARTICLE INFO

Keywords: Deforestation; Forest Ecosystems; Land Use; Natural Resources.

Received : 02 July 2022

Revised : 30 August 2022

Accepted : 31 August 2022

ABSTRACT

The anthropization of forest ecosystems has become a major environmental problem with negative impacts on biodiversity around the world. Responding to such a problem requires monitoring land use. Thus, this study aims to analyze the Spatio-temporal dynamics of land use (LULC) to implement effective management strategies for forest ecosystems in the South Talihya watershed in eastern DR Congo. For this, a diachronic study of Landsat TM+ satellite images from 1987 and 2001 and Sentinel-2 from 2020 was used. The results revealed that natural formations have regressed in favor of croplands and fallow mosaics in the Talihya South watershed. The forests which occupied 183.68 km² in 1987, decreased to 140.94 km² in 2001 and 108.2 km² in 2020. Bare lands and buildings represented 87.54 km² in 2020 against 115.33 km² in 2001 and 58.63 km² in 1987. The current state of land use indicates that Crop lands, fallows, and pastures occupy a high surface area compared to forests and bare lands and buildings. These Crop lands, fallows, and pastures occupied 317.88 km² in 1987, 303.74 km² in 2001, and 373.34 km² in 2020. The observed changes result from overexploitation of resources characterized by the expansion of agricultural lands and tree logging. The annual deforestation rate calculated from forested areas of Talihya South watershed between dates t_0 (1987) and t_1 (2020) was 1.60%. In view of these results, participatory land use planning is a way to ensure sustainable management of the existing residual forests in this watershed.

INTRODUCTION

The forest cover of the Democratic Republic of Congo (DR Congo) is over 166 million hectares and alone accounts for more than 62% of the Congo basin's forest cover, which is 69% dense forest as opposed to approximately 30% only of other forest types (Tchatchou et al., 2015). These forested formations in DR Congo cover about 54.6% of its surface area (Nsangua et al., 2018). These forests are also at risk of degradation not only due to illegal tree logging, but mainly following slash-and-burn

cultivation for food production, inducing an annual loss of 532,000 of forest cover (Hatakiwe, 2016).

These dense tropical forests of the Congo Basin host tremendous biodiversity, constitute a source of food and livelihood for more than 60 million people and about 44 million hectares are under forest exploitation regimes as forest concessions (Megevand et al., 2013; Manguiengha et al., 2019). The primary causes of deforestation include but not limited to slash-and-burn agriculture, timber logging, the increasing need for

fuelwood, and wildfires (Hami et al., 2007; Megevand et al., 2013; Sylla et al., 2019). These factors of deforestation and forest degradation result in changes in vegetation structure and floristic composition of the landscape (Sylla et al., 2019). According to Gebhardt et al. (2015), the intensification of activities over time has generated significant remodeling, not only of the forest cover but also of the underlying soil.

The drivers of deforestation in Lubero territory are similar to those reported in the tropical zone in general. This eco-region is characterized by the scarcity of forested areas, as a direct consequence of deforestation since the 18th century through the field and pastures establishment (Vyakuno, 2006). The watershed drained by the South Talihya River is situated in the cool highlands of Lubero, densely populated with a decreasing forest cover in the market gardening area extending from Kyondo to Masereka. The remaining forests in this zone are in form of forest refuges or forest fragments (Vyakuno, 2006), indicating anthropization in these areas. Some areas that have been deforested for centuries are struggling to evolve towards the mountain forest climax and remain at the savanna stage because of the climate and repetitive bushfires that slow down spontaneous reforestation (Vyakuno, 2006). In this context of demographic pressure, it is necessary to know the trends of the dynamics of the forest cover over time as well as its underlying drivers for informed decision-making (Akakpo et al., 2017). This raises the question of sustainable resource management in this watershed, which is the epicenter of market garden production that serves the proximate cities of Butembo and Beni.

The development of remote sensing and geographic information system (GIS) techniques allows for an increasingly precise approach to assessing land use dynamics (Oloukoi et al., 2006; Kpedenou et al., 2016). Remote sensing and GIS, which are not only increasingly used for the study of phenomena occurring on the earth's surface, form essential tools in interactive decision support systems (Diedhiou et al., 2020). This study examines the dynamics of land use in the South Talihya watershed. The mapping of land use and land cover changes are real tools for planning and decision-making support, especially in the

management and preservation of natural resources and ecosystems.

MATERIALS AND METHODS

Study Site

The study was conducted in the South Talihya River watershed. This watershed is located in the Cool Highlands of Lubero, in the North-East of the DR Congo. These Cool Highlands are located between 2000 and 3100 m of altitude have schistose and granitic rocks from the Precambrian period and relief of dissected and abrupt hills. The annual averages of temperature and precipitation are low due to the altitude: 15 to 17 °C and 1,110 to 1,330 mm. The forest is mountainous with orophilous species. The lower limit of this stage has as agronomic indicators potatoes and wheat that grow well only above the 1800 m isohypse (Kasay, 1988; Vyakuno, 2006). The South Talihya River originates south of Masereka and flows south before turning east to flow directly into Lake Edouard. Its basin offers the juxtaposition of different forms corresponding to different erosion cycles (Vyakuno, 2006). The South Talihya watershed is populated by the *Nande*, the largest ethnic group traditionally known as *Yira*. The economy of the region is based on subsistence agriculture that is carried out by resource-poor farmers.

Choice of satellite images, dates, and Acquisition of satellite images

To study the dynamics of land use, Landsat images were used. Since the landscape of the South Talihya watershed is highly fragmented, the 2020 Sentinel-2 image was also used to improve the accuracy of the classification.

Compared to Landsat data, the revisit time of the satellite of 16 days does not allow under certain conditions to optimize the chances of having several images in a short time for monitoring and to avoid the problem induced by the presence of clouds, recurrent in the tropical context. Following this bottleneck, the development of the ESA Copernicus program since 2015 has offered new Sentinel-2 optical images with improvements in spatial resolution (10 to 60 m) and the revisit time of the satellites (5 days). With the short revisit time, Sentinel-2 imagery allows better monitoring of vegetation and better management of cloud-induced problems (Konko et al., 2021).

Considering the specific characteristics of each satellite image and their availability, two Landsat scenes were used, one from 1987 and the other from 2001 (Enhanced Thematic Mapper+: ETM+). For 2020, the Sentinel-2 image with a resolution of 10 m was used to study the spatial dynamics of soil cover in the South Talihya watershed. The choice of dates was based on data availability and quality. In addition, we tried to coincide these dates with key dates in the development of the region. The spatial resolution of these images is 30 meters, of UTM zone 35 S projection with WGS84 reference ellipsoid. Landsat images were downloaded during the period marked by little rainfall. In fact, Hountondji (2008) and Akakpso *et al.* (2017) suggest that the driest months of the year are the most favorable period for vegetation characterization by spatial remote sensing. The

images acquired during such periods are not very cloudy (Agbanou, 2018) and allow for to generate of bio-environmental and geographical information close to the reality of the field (Hountondji, 2008; Oszwald *et al.*, 2012; Akakpso *et al.*, 2017; Agbanou, 2018).

Landsat satellite images were downloaded from the Earth Explorer website (<https://earthexplorer.usgs.gov/>) in geoTiff format, selecting those with the least amount of disturbance, especially cloud cover. The 2020 Sentinel-2 image was downloaded from <https://visioterra.org/VtWeb/>. The Radar (SRTM) images, essential for the delineation of the studied watershed, were downloaded from <http://dwtkns.com/srtm>. The characteristics of the satellite images used are described in Table 1.

Table 1. Characteristics of the scenes

Capteur	Date d'acquisition	Résolution spatiale (m)	Path/Row	Projection
Landsat 5-TM	1987-08-07	30x30	173/060	UTM/ WGS84, 35 N-S
Landsat 7-ETM+	2001-03-14	30x30	173/060	UTM/ WGS84, 35 N-S
Sentinel-2	2020-06-01	10x10	-	UTM/ WGS84, 35 N-S

Preprocessing of satellite images

1. Color composition and filtering

The color composition was done depending on each image scene. The images were visualized in

true colors or in false colors according to the need. An example of a color composition for the images used in this study is illustrated in Figure 1.



Figure 1. 2001 Landsat ETM+ image true color composition: 3, 2, 1. The capture of an area situated on the escarpments of Lake Edward in the South Talihya watershed.

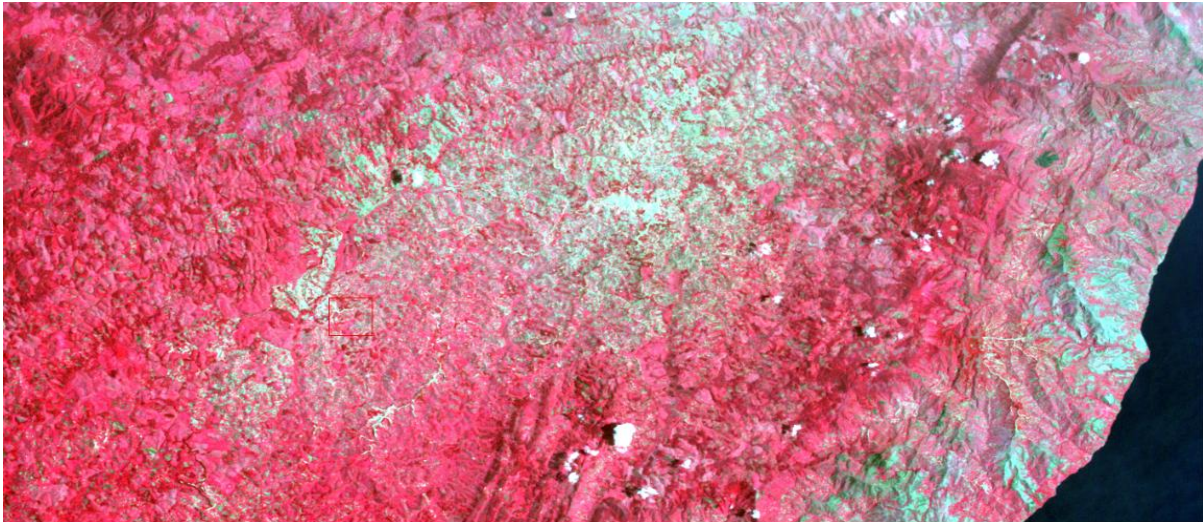


Figure 2. 2001 Landsat ETM+ image false color composition: 4, 2, 1. The capture of an area situated on the escarpments of Lake Edward in the South Talihya watershed.

From the true color composition (Figure 1), the land use classes appear with natural colors: water appears in blue, woody vegetation appears in dark green, cultivated land and fallow land in light green and finally bare and built-up land in gray. In contrast, in false color (Figure 2), water is black, tree vegetation with high chlorophyll intensity is dark red, and cultivated lands and fallow lands are light red. The whitish spots visible in both images are the clouds. Once the color composition was done for each image, we performed a Gaussian filter which allowed the elimination of the isolated pixels and homogenized the thematic classification.

2. Extraction of the study areas

To prevent bias in the classification, areas of interest were extracted on the scene of the satellite image used. This extraction was done from the multispectral images obtained, following the boundaries of the South Talihya watershed using the Resize data tool in Basic Tools of ENVI software version 4.6.

3. Resampling

Resampling of the pixels was applied because the images (Landsat 5 ETM+ and Sentinel-2) did not have the same spatial resolution. This operation allows them to be superimposed during the implementation of the transition matrix. In addition to radiometric improvements, the Landsat images underwent geometric corrections that consisted of realigning the image to a geographic reference frame (Dolbec et al., 2005; Katembera Ciza et al., 2015; Tsewoue et al., 2020). The nearest neighbor resampling method was adopted in this study. This

method uses the nearest pixel value without any interpolation to create the rectified pixel value. Therefore, the radiometric values of the pixels are not affected during resampling (Sagne et al., 2015).

Image classification

The supervised classification method was implemented for the processing of Landsat images. The Maximum Likelihood (ML) algorithm was chosen for image classification. This algorithm assigns each pixel to the class to which it has the highest probability of belonging (Katembera Ciza et al., 2015; Agbanou et al., 2018; Orekan et al., 2019; Manguiengha et al., 2019) by highlighting the standard error range between pixel values and those of different training sites (ROIs) (Orekan et al., 2019). The established classification as well as the representation colors of each land cover category were adapted from the Corine Land Cover (CLC) nomenclature (Agbanou et al., 2018; Mbaiyetom et al., 2020). The classification of the 2020 Sentinel-2 image was done based on ground data from the same year, whereas the classification of the 1987 and 2001 Landsat images was done retrospectively and deductively (based on the spectral similarity of the 2020 Sentinel-2 image classes, due to the lack of ground data for these years). For each land cover class, ROIs (training areas) were delineated away from transition areas to avoid including mixed pixels that could be classified into two separate classes. The definition of the training areas (ROIs) on the Sentinel-2 image is shown in Figure 3 below.

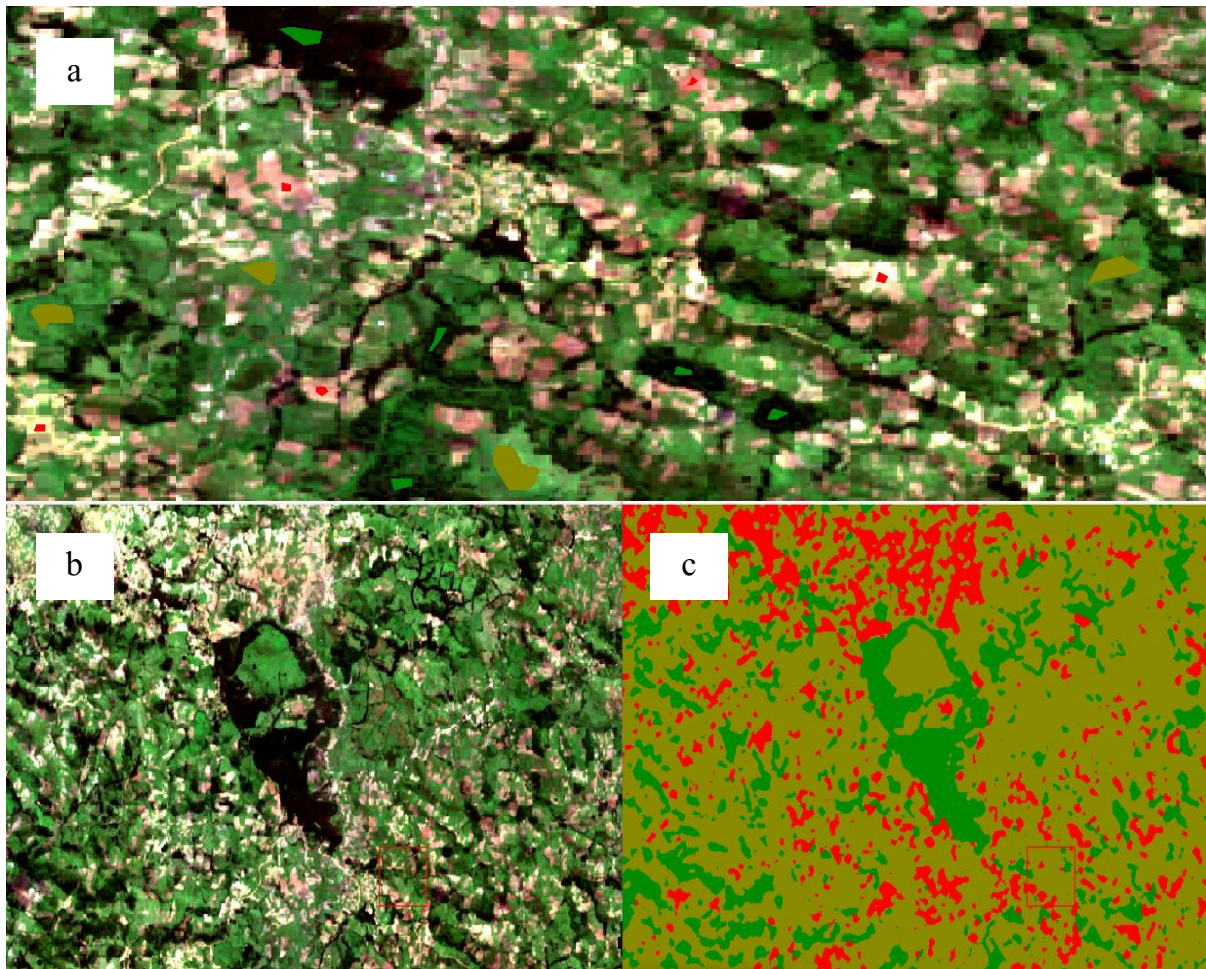


Figure 3. Delineation of training areas or regions of interest (ROI) based on land cover classes (a), unclassified Sentinel-2 image (b), and maximum likelihood classification image (c)

From the ground data, three land cover classes were identified: Forest (including forest residuals and tree plantations), Mosaic fields and fallows (including croplands and herbaceous fallows), Savannahs (including grassy formations interspersed with shrubs), and Bare lands and built-up soils (including plowed fields, roads, and built-up areas). For each occupation class, georeferenced points constituting “training areas” were used for verification. These coordinates had a spatial distribution over the entire study area as suggested by Adjonou et al. (2019). For Tsewoue et al. (2020), ground truth missions allow the validation of the boundaries of the different land use classes resulting from the interpretation and influence the accuracy of the classification. In this phase, vectorization was executed on the classified images. These were transformed into a *Shapefile* to determine the surface areas of each land use class.

Classification accuracy and validation

The accuracy of the classifications obtained in this paper was evaluated through the use of a confusion matrix or contingency table. For Randriamalala (2015), the confusion matrix is one of the most used statistical indicators in the performance of classification. It highlights the confrontation between the results of the supervised classification and the reference data that represent the ground truth (Soulama et al., 2015; Rifai et al., 2018; Okanga-Guay et al., 2019; Orekanet al., 2019; Gbedahi et al., 2019; Useni Sikuzani et al., 2020). In fine the model accuracy indicators (overall accuracy (OA), User accuracy (UA), Producer accuracy (PA), omission errors, and commission errors) were calculated from the confusion matrixes obtained by cross-validation. The validation of the classification was based on the Kappa index, which was assessed by means of a confusion matrix. This coefficient incorporates all the elements of the confusion matrix (Hountondji,

2008) and characterizes the ratio between the number of well-ranked pixels and the total pixels sampled (Kpedenou et al., 2016; Cabala Kaleba et al., 2017; Fotso et al., 2019; Adjonou et al., 2019). It is given by the following formula (Bekele et al., 2021):

$$K = \frac{N \sum_{i=1}^r X_{ii} - \sum_{i=1}^r (x_i + (x+i))}{N^2 - \sum_{i=1}^r (x_i + (x+i))} \dots\dots (1)$$

With r=number of rows in the matrix; X_{ii}= number of observations in row i and column i (diagonal elements); x_i+ and x_i+ = represents the marginal total of rows r and columns i and N= number of observations. The Kappa coefficient, which varies from 0 to 1 (Orekan et al., 2019) and reflects a level of concordance that is all the higher the closer its value is to 1 (Hountondji, 2008). It is divided into five categories: very low agreement from 0 to 0.20; low agreement from 0.21 to 0.40; moderate agreement from 0.41 to 0.60; substantial agreement from 0.61 to 0.80; and almost perfect agreement from 0.81 to 1 (Landis and Koch, 1977). A study can be validated if the Kappa index is between 50% and 75% (Cabala Kaleba et al., 2017).

Analysis of land cover change

The classified images were transformed into a shapefile so that the areas of each land use unit could be calculated. This made it possible to establish the transition matrix as recommended by Schlaepfer (2002). It allows to highlight in a way the different forms of conversion undergone by the land use units between two dates t₀ and t₁, and to describe the changes that occurred (Kpedenou et al., 2016; Avakoudjo et al., 2014; Arouna et al., 2016; Toko Imorou et al., 2019; Oloukoi et al., 2006; Avakoudjo et al., 2014; Ayena et al., 2017; Samba et al., 2021; Bamba et al., 2008).

The transition matrix is in the form of a square matrix and consists of X rows and Y columns (Avakoudjo et al., 2014; Arouna et al., 2016; Toko Imorou et al., 2019). The number of rows in the matrix indicates the number of land use units at

time t₀ (1987), the number Y of columns in the matrix is the number of converted units at time t₁ (2020), and the diagonal contains the areas of the units that remained unchanged (Oloukoi et al., 2006; Avakoudjo et al., 2014; Ayena et al., 2017; Samba et al., 2021). The transformations are done from rows to columns (Toko Imorou et al., 2019; Samba et al., 2021). The cells of the matrix contain the value of a variable that moved from an initial class i to a final class j during the period from t₀ to t₁. Column and row values represent the proportions of the areas occupied by each land use class at the corresponding time (Bamba et al., 2008; Ayena et al., 2017).

The annual deforestation rate was calculated for the period under consideration. The standardized formula proposed by Puyravaud et al. (2002) was used to calculate the annual deforestation rate:

$$T (\%) = \frac{1}{t_1 - t_0} \ln \left(\frac{S_1}{S_0} \right) * 100 \dots\dots (2)$$

With

- S₀ = initial year's forest area
- S₁ = forest area of the final year
- t₀ = exact acquisition date of the image for the initial year
- t₁ = exact acquisition date of the image for the final year

RESULTS AND DISCUSSION

Confusion matrices and Kappa indices

The confusion matrix for the classification of the 1987 Landsat image reveals that 99.24% of the pixels in the class “Crop Lands, Pastures and Fallows” were well classified (Table 2). For the classes “Bare lands and buildings” and the class “Forests”, all pixels were accurately classified. Only 0.51% of pixels in the class “Crop Lands, Pastures and Fallows” were confused with those in the class “Bare lands and Buildings”. Overall, the results of the confusion matrix are acceptable.

Table 2. Confusion matrix of the year 1987 classification in percentage of pixel

LULC	Bare lands and buildings	Crop Lands, Fallows, and Pastures	Forests	User Accuracy
Unclassified	0	0	0	
Bare lands and buildings	100	0.51	0	99.46
Crop Lands, Fallows, and Pastures	0	99.24	0.33	96.78
Forests	0	0.25	99.67	99.97
Total	100	100	100	
Producer Accuracy	100	99.24	99.67	

The overall classification accuracy of the 2001 image is 99.57% and the Kappa index is 0.98 (Table 3).

Table 3. Confusion matrix of the year 2001 classification in the percentage of pixel

LULC	Crop Lands, Fallows, and Pastures	Bare lands and buildings	Forests	User Accuracy
Unclassified	0	0	0	
Crop Lands, Fallows, and Pastures	99.46	0	0	100
Bare lands and buildings	0.54	100	0	93.33
Forests	0	0	100	100
Total	100	100	100	
Producer Accuracy	99.46	100	100	

In the class “Crop lands, Pastures and Fallows” ,99.46% of the pixels were well classified. For the classes “Bare lands and Buildings” and the class “Forests”, all pixels were accurately classified. The percentage of pixels in the class “Crop lands, Pastures and Fallows” that were confused with those in the class “Bare lands and buildings” is 0.54%. Overall, the results of the confusion matrix are satisfactory.

The overall accuracy of the classification of the 2020 Sentinel-2 image is 99.61% while the Kappa index obtained is 0.99. The confusion matrix

of the classification of this Sentinel-2 image is summarised in Table 4. According to the confusion matrix (Table 4), the classification was successful because the confusions between the different land use classes are low, with the exception of 0.81% of the pixels of the class “forests” which were confused with the pixels of the class “Crop lands, pastures, and fallows”. In general, these results are acceptable because the South Talihya watershed is situated in an anthropized area where the clear distinction of land use classes is not very evident.

Table 4. Confusion matrix of the year 2020 classification in the percentage of pixel

LULC	Forests	Croplands, pastures, and fallows	Bare lands and buildings	User Accuracy
Unclassified	0	0	0	
Forests	99.19	0	0	100
Croplands, pastures, and fallows	0.81	100	0	98.89
Bare lands and buildings	0	0	100	100
Total	100	100	100	
Producer Accuracy	99.19	100	100	

Pixel omission and commission errors

The percentages of pixel omission (Om) and commission (Com) errors in the classification of the 1987 Landsat image are reported in Table 5.

Table 5. Pixel omission and commission errors from the South Talihya watershed classification

LULC	1987		2001		2020	
	Com (%)	Om (%)	Com (%)	Om (%)	Com (%)	Om (%)
Bare lands and buildings	0.54	0	6.67	0	0	0
Croplands, fallows, and pastures	3.22	0.76	0	0.54	1.11	0
Forests	0.03	0.33	0	0	0	0.81

From the results in Table 5 (year 1987), the percentages of omission errors in the land use classes are low. The omission errors for the 'Fields, fallows and pastures' class represent only 0.76% while for the “forests” class, they represent 0.33%. For the class “Crop lands, fallows and pastures”, the errors of the commission represent 3.22%, which is also low and not likely to taint the results of the classification. The results in Table 5 (year 2001), the percentages of omission errors in the land use classes are low. The errors of omission for the class “Crop lands, fallows and pastures” represent only 0.54%. For the class “Bare lands and buildings”, the errors of the commission represent 6.67%, which is also low and not such as to taint the results of the

classification. The results reported in Table 5 (year 2020) show that 0.81% of the pixels in the “forests” class were omitted while the commission rate is 1.11% for pixels in the “Crop lands, fallows, and pastures” class.

Dynamics of land cover between 1987 and 2020

The class “cropland, fallows, and pastures” was always the most dominant but decreased slightly between 1987 and 2001 before rising up in 2020. On the contrary, the “Bare land and buildings” class increased between 1987 and 2001 before dropping again in 2020. The class “forest” on its behalf is consistently decreasing from 1987 to 2020 (Figure 4).

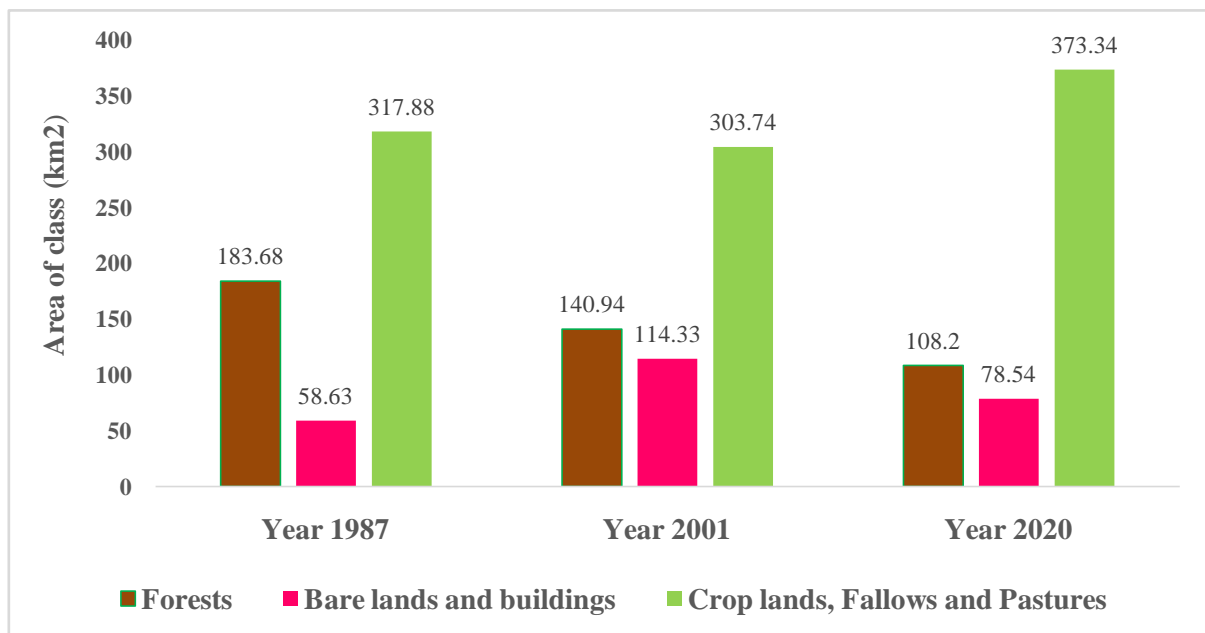


Figure 4. Area of land use classes as a function of years

The land cover maps (1987, 2001, and 2020) in the South Talihya watershed are illustrated in Figure 5.

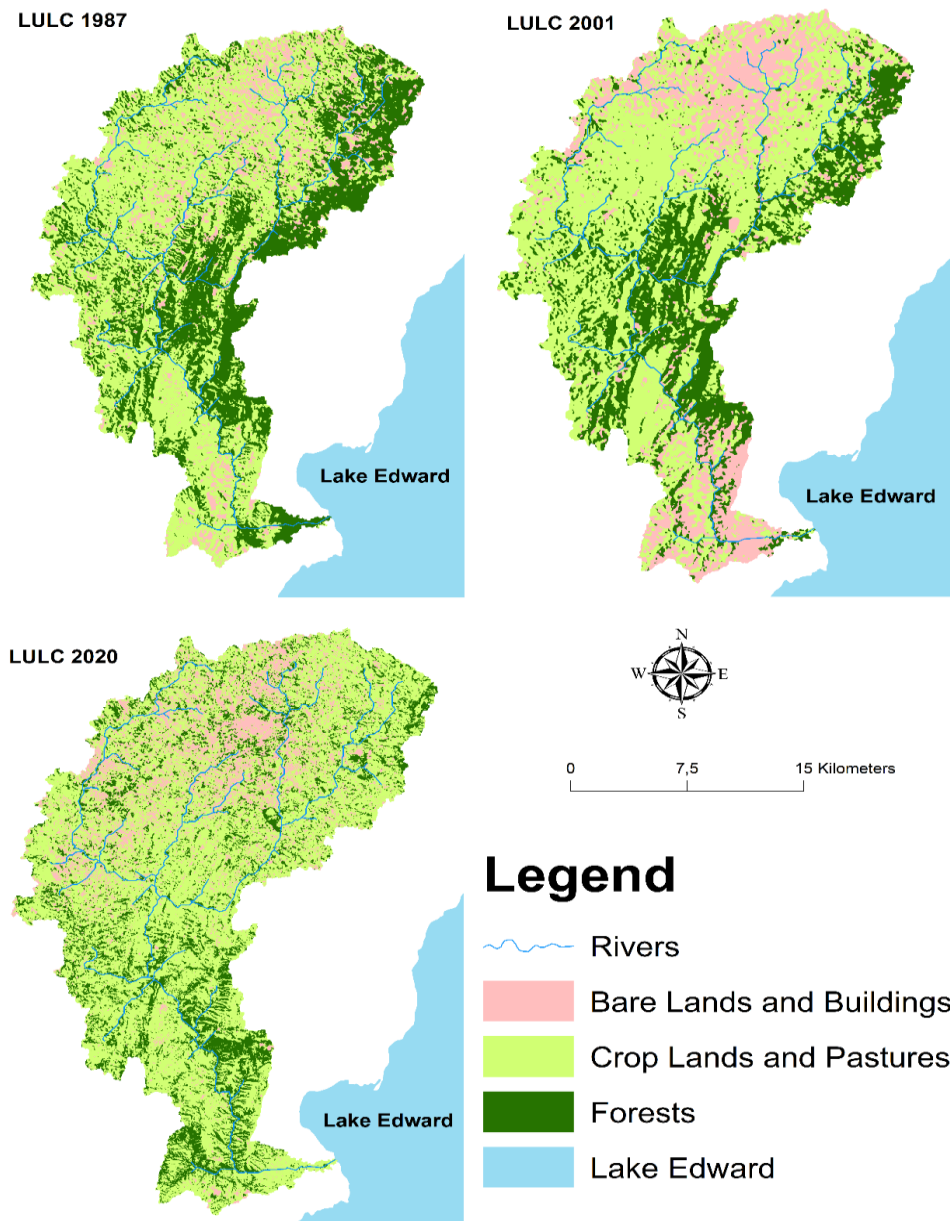


Figure 5. Land use maps of the South Talihya watershed

Land Use Changes between 1987 and 2020

The values in the transition matrices below are presented as percentages of area. For ease of interpretation, the total area of the South Talihya watershed is estimated to be 560.5 km², so 1% is approximately 5.605 km².

The land use transition matrix in the South Talihya Watershed between 1987 and 2001) shows that bare lands and buildings increased from 10.48% in 1987 to 20.45% in 2001 (Table 6). Croplands, fallows, and pastures, on the other hand, increased from 56.76% in 1987 to 54.34% in 2001. In this watershed, forests decreased from 32.76% in 1987 to 25.21% in 2001. The results show that out

of 20.45% in 2001, 4.37% was forests in 1987 while out of 54.34% of Crop lands, fallows, and pastures in 2001, 10.43% was forests in 1987. In contrast, the changes between 2001 and 2020 (Table 7) are such that Crop lands, fallows, and pastures have increased significantly from 54.34% in 2001 to 66.65% in 2020. As between 1987 and 2001, forests have decreased from 25.23% in 2001 to 19.31% in 2020. The transition matrix also shows that of the 66.65% of Crop lands, fallows, and pastures in 2020, 16.18% were forests in 2001, and of the 19.31% of forests in 2020, 8.01% were Crop lands, fallows, and pastures in 2001.

Table 6. Land use transition matrix in the South Talihya watershed between 1987 and 2001

2001 \ 1987	Bare lands and buildings	Croplands, fallows, and pastures	Forests	Total
Bare lands and buildings	4.08	12.00	4.37	20.45
Croplands, fallows, and pastures	5.68	38.23	10.43	54.34
Forests	0.72	6.53	17.97	25.21
Total	10.48	56.76	32.76	100.00

Table 7. Land use transition matrix in the South Talihya watershed between 2001 and 2020

2020 \ 2001	Bare lands and buildings	Croplands, fallows, and pastures	Forests	Total
Bare lands and buildings	4.72	8.10	1.23	14.05
Croplands, fallows, and pastures	12.24	38.23	16.18	66.65
Forests	3.48	8.01	7.82	19.31
Total	20.45	54.34	25.21	100.00

The annual deforestation rate calculated from the forest areas at date t0 (1987) and t1 (2020) is 1.60% for the South Talihya watershed.

Evaluation of the quality of classifications

The Maximum Likelihood classification algorithm gave good results. The preference of this classification method is due to its qualities related to its robustness in identifying classes that are spectrally close enough (Oszwald et al., 2010; Soro et al., 2013), which offers a good generalization capacity (Tente et al., 2019). It has given good results during the work of several authors (Soro et al., 2013) by the fact that it assigns each pixel to the class to which it has the highest probability of belonging (Katembera Ciza et al., 2015; Agbanou et al., 2018; Orekan et al., 2019; Manguiengha et al., 2019; Samba et al., 2021) by highlighting the standard margin of error between pixel values and those of different training sites (ROI) (Orekan et al., 2019).

The implementation of this supervised image classification with three classes for South Talihya gave very good Kappa index values (higher than 75%) based on the rating scale proposed by Landis and Koch (1977). According to Landis & Koch (1977) and Kundell & Polansky (2003), this index is “Excellent” when it is greater than or equal to 81%; “Good” when it is between 80% - 61%; “Moderate” when it is between 60% - 41%; “Poor” when it is between 20%- 0%, and “Very Poor”

when it is less than 0%. Pontius (2000); Oloukoi et al. (2006); Cabala Kaleba et al. (2017) demonstrated that a land-use study can be validated if the Kappa index is between 50% and 75%. Thus, the values of the Kappa index obtained in this study are in the range of 0.75 to 1 which is estimated as satisfactory in the framework of a maximum likelihood assisted classification for the tropical region (Sangne et al., 2015; Agbanou, 2018). Given the complexity of the landscape in these two watersheds, such a result can be explained by the quality of the images and the choice of thematic classes and training areas guided by the ground truth. In addition, the use of the 2020 Sentinel-2 image also contributed to the improvement of the classification quality.

According to Adjonou et al. (2019), the Sentinel-2 image shows better performance in the discrimination of land cover types. Although Cohen's Kappa index is widely used in works on land cover dynamics for classification validation (Barima et al., 2009; Kyale Koy et al., 2019), it is subject to many criticisms related to its misuse (Agbanou, 2018). This index is normally used in the case of systematic sampling, carried out randomly (Golden, 2006). However, despite the opinions tending to question the quality of the precision provided by Cohen's Kappa index, no index has yet been able to validly replace it in terms of evaluation and validation of the results obtained following the

supervised classification of the different land use units (Agbanou, 2018).

Change In Land Cover and Deforestation Rates In The Watershed Between 1987 and 2020

The annual deforestation rate is 1.60% for the South Talihya watershed and is lower than the rate reported by Ndavaro et al. (2021) who found an annual deforestation rate of 2.2% in the Cool Highlands of Lubero. A slightly higher annual deforestation rate of 2.7% was obtained by Bweya et al. (2019) in the Beni region. This difference in annual deforestation rate with Bweya et al. (2019) and Ndavaro et al. (2021) may be due to the influence of the observation scale.

The values of the annual deforestation rate estimated at the South Talihya watershed in this study are much higher than those obtained in the Congo Basin. Ernest et al. (2010) found that the deforestation rate in DR Congo doubled from 0.15% in 1990-2000 to 0.22% in 2000-2005. Debroux et al. (2007) on their behalf reported 0.4% annual deforestation rate between 1984 and 1998 against an average annual deforestation rate of 0.6% between 1990 and 1995 in the tropics (Herve et al., 2015). Around the Yangambi Biosphere Reserve, Kyale Koy et al. (2019) estimated the annual net deforestation rate to be 0.18% while a value of 0.13% was obtained by Katembera Ciza et al. (2015) around the Yangambi Biosphere Reserve. These contrasting deforestation rates reveal that the global average hides strong disparities between particular regions (Debroux et al., 2007). But also, the divergence of data sources and processing methods, added to the difficulties of collection and harmonization, often lead to notable differences in the different evaluations of deforested areas (Herve et al., 2015). In addition, Yangambi Biosphere Reserve is a conservation area where human activities are limited. This may suggest that the annual deforestation rate is low compared to the South Talihya watershed where population density is high and land use activities are mainly agricultural and pastoral.

In addition, the analysis of the dynamics of change in land use classes in the South Talihya watershed has highlighted the various processes of evolution that occurred in the landscape during the period 1987-2020. These changes are mainly related to the regression of natural formations (deforestation process) such as dense forest

formations in favor of Crop-fallows mosaics and bare lands and buildings areas that have also increased in the area. The factors most commonly cited as having strongly contributed to the reduction of forest and savanna areas include inappropriate agricultural practices, logging and charcoal production, and vegetation fires (Vyakuno, 2006; Adjonou et al., 2013). In this watershed, the manifestations of these factors are increasingly felt with the ever-increasing population growth in the area, thus increasing tenfold the need for croplands and increasing the pressure on natural resources (Vyakuno, 2006).

CONCLUSION

The objective of this paper was to study the dynamics of land use in the watershed of the South Talihya River. The results reveal that this dynamic of land use has led to the decrease of forest areas in favor of agricultural lands and fallows. Therefore, the rational management of natural resources in this agropastoral area and the restoration of forest ecosystems in this watershed with a high population density is necessary. This rational management will require a holistic approach to integrate a wide range of parameters and will guarantee sustainable development, a guarantee of a fulfilling life where the risk approach is integrated into the spatial planning process whose unit is the watershed.

REFERENCES

- Adjonou, K., Bindaoudou, I.A-K., Idohou, R., Salako, V.K., Glele-Kakai, R. & Kokou, K. (2019). Suivi satellitaire de la dynamique spatio-temporelle de l'occupation des terres dans la réserve de biosphère transfrontalière du Mono entre le Togo et le Bénin de 1986 à 2015. In *Actes de la conférence scientifique internationale*, 13–15 mars 2019, Hôtel Azalai, Cotonou, Bénin.
- Agbanou, B.T. (2018). Dynamique de l'occupation du sol dans le secteur Natitingou-Boukombé (Nord-Ouest Bénin): De l'analyse diachronique à une modélisation prospective. *Thèse de doctorat*, Université Toulouse-Jean Jaurès et Université d'Abomey-Calavi.
- Agbanou, B.T., Orekan, V., Djafarou, A., Paegelow, M. & Tente, B. (2018). Dynamique spatio-temporelle de l'occupation du sol en zone d'agriculture

- extensive: cas du secteur Natitingou-Boukoumbe au Nord-Ouest du Bénin. Mélanges en hommage aux professeurs Thomas Omer, Houssou Sègè Christophe et Houndaga Cossi Jean. La géographie au service du développement durable, Septembre 2018, Abomey-Calavi, Bénin.
- Akoma Miyono, J.A.J., Makak, J-S., Palla, F. & Trebossen, H.F.M. (2019). Images satellites pour l'évaluation de l'occupation du sol dans les sites de gestion au Gabon. In *Actes de la conférence scientifique internationale*, 13–15 mars 2019, Hôtel Azalaï, Cotonou, Bénin.
- Arouna, O., Etene, C.G. & Issiako, D. (2016). Dynamique de l'occupation des terres et état de la flore et de la végétation dans le bassin supérieur de l'Alibori au Bénin. *Journal of Applied Biosciences* 108: 10543-10552.
- Avakoudjo, J., Mama, A., Toko, I., Kindomihou, V. et Sinsin, B. (2014). Dynamique de l'occupation du sol dans le Parc National du W et sa périphérie au nord-ouest du Bénin. *Int. J. Biol. Chem. Sci.* 8(6), 2608-2625.
- Ayena, A.A., Totin, H.S.V., Amoussou, E. & Vissin, E.W. (2017). Impact de la dynamique de l'occupation du sol sur les berges dans la vallée du fleuve Niger au Bénin. *Rev. Ivoir. Sci. Technol.*, (29), 119 – 135.
- Bamba, I., Mama, A., Neuba, D.F.R., Koffi, K.J., Traore, D., Visser, M., Sinsin, B., Lejoly, J. & Bogaert, J. (2008). Influence des actions anthropiques sur la dynamique spatio-temporelle de l'occupation du sol dans la province du Bas-Congo (R.D. Congo). *Sciences & Nature*, 5, (1), 49-60 .
- Barima, Y.S.S., Barbier, N., Bamba, I., Traore, D., Lejoly, J. & Bogaert, J. (2009). Dynamique paysagère en milieu de transition forêt-savane ivoirienne. *Bois et forêts des tropiques*, 1 (299), 25-25.
- Bekele D.A., Gella G.W. & Ejigu M.A. (2021). Erosion risk assessment: A contribution for conservation priority area identification in Lake Tana sub basin, NW Ethiopia, *International Soil and Water Conservation Research*, 10 (1), 46-61.
- Cabala Kaleba, S., Useni Sikuzani, Y., Sambieni, K.R., Bogaert, J. & Munyemba Kankumbi (2017). Dynamique des écosystèmes forestiers de l'Arc Cuptifère Katnagais en République Démocratique du Congo. I. Causes, transformations spatiales et ampleur. *Tropicultura*, 35 (3), 192-202.
- Debroux, L., Hart, T., Kaimowitz, D., Karsenty, A. & Topa, G. (Eds.) (2007). La forêt en République Démocratique du Congo Post-conflit: Analyse d'un Agenda Prioritaire. Rapport collectif, 82.
- Diedhiou, I., Mering, C., Sy, O. & Tidiane Sane, T. (2020). Cartographie par télédétection l'occupation du sol et ses changements, *EchoGéo*, (54), 1-41.
- Dolbec, J-F., Rousseau, A.N. & Quilbe, R. (2005). Développement d'un processus de classification d'images satellitaires afin de détecter les changements d'occupation du sol sur le bassin versant de la rivière Chaudière pour la période 1970 à 2000 : Exemple de l'image Landsat-5 du 6 août 1987. Rapport pour le projet: FACCA9446, n°802. Programme Impacts et Adaptation, Québec, 85.
- Ernst, C., Verhegghen, A., Mayaux, P., Hansen, M. & Defourny, P. (2010). Cartographie du couvert forestier et des changements du couvert forestier en Afrique centrale. In *Etat de forêts du Bassin du Congo*. Luxembourg: Office des Publications de l'Union Européenne.
- Fotso, R., Fosso, B. & Mbenda, G.N. (2019). Évolution du couvert végétal du Parc National Mbam et Djerem et sa périphérie entre 2000-2018. In *Actes de la conférence scientifique internationale*, 13–15 mars 2019, Hôtel Azalaï, Cotonou, Bénin.
- Gbedahi, O.L.C., Biao, S.S.H., Mama, A., Gouwakinnou, G.N. & Yorou, N.S. (2019). Dynamique du couvert végétal à Bassila au nord Bénin pendant et après la mise en œuvre d'un projet d'aménagement forestier. *Int. J. Biol. Chem. Sci.* 13(1), 311-324.
- Golden, C. (2006). Influence du choix des parcelles d'apprentissage et de validation sur la qualité des résultats de classifications supervisées orientées objet d'images de télédétection. *Sciences de l'environnement, Montpellier*, 73 p.
- Hatakiwe, R.H. (2016). *Etude floristique et structurale comparée de la strate des dominés de la forêt monodominante à*

- Gilbertiodendron dewevreii* J. Leonard et de la forêt mixte à *Scorodophloeus zenkeri* Harms dans la réserve forestière de la Yoko. Mémoire de licence en agronomie générale, UNIKIS, 53 p.
- Herve, D., Razanaka, S., Rakotondraompiana, S., Rafamantanantsoa, F. & Carriere, S. (eds.) (2015). Transitions agraires au sud de Madagascar. Résilience et viabilité, deux facettes de la conservation. Actes du séminaire de synthèse du projet FPPSM Forêts, Parcs, Pauvreté au sud de Madagascar, 10-11/06/2013, Antananarivo, IRD-SCAC/PARRUR, Ed. MYE, 366 p.
- Hountondji, Y.-C.H. (2008). Dynamique environnementale en zones sahélienne et soudanienne de l'Afrique de l'Ouest: Analyse des modifications et évaluation de la dégradation du couvert végétal. Thèse de doctorat en Sciences, Université de Liège, 153 p.
- Jofack Sokeng, V.C., Akpa, Y.L., Assoma, T.V., Kouame, K.F., Corgne, S., Rudant, J.-P., Ouattara, T.A., Sorho, F.M., Yao, N. & Kouame, N.P. (2019). Suivi par télédétection des affectations des terres pour la promotion d'une agriculture intégrée au développement forestier en Côte d'Ivoire. In Actes de la conférence scientifique internationale, 13-15 mars 2019, Hôtel Azalaï, Cotonou, Bénin.
- Kasay, K. (1988). *Dynamisme Démo-Géographique et mise en valeur de l'Espace en milieu équatorial d'altitude : Cas du Pays Nande au Kivu Septentrional, Zaïre. Thèse Doctorat en Géographie*. Université de Lubumbashi, Lubumbashi.
- Katembera Ciza, S., Mikwa, J.-F., Cirhuza Malekezi, A., Gond, V. & Boyemba Bosela, F. (2015). Identification des moteurs de déforestation dans la région d'Isangi, République démocratique du Congo. *Bois et forêts des tropiques*, 2 (324), 29-38.
- Koumoi, Z., Alassane, A., Djangbedja, M., Boukpepsi, T. & Kouya, A.-E. (2013). Dynamique spatio-temporelle de l'occupation du sol dans le centre-Togo. AHOHO- Revue de Géographie du LARDYMES, Université de Lomé, 7 (10), 163-172.
- Kpedenou, K.D., Boukpepsi, T. & Thiou Tanzidani K. Tchamie (2016). Quantification des changements de l'occupation du sol dans la préfecture de Yoto (Sud-est Togo) à l'aide de l'imagerie satellitaire LANDSAT. *Revue des Sciences de l'Environnement, Laboratoire de Recherches Biogéographiques et d'Etudes Environnementales (Université de Lomé)*.
- Kundel H.L. & Polansky M. (2003). Statistical Concepts Series Radiology. Measurement of Observer Agreement, *Radiology*, 228 (2), 303-308.
- Kyale Koy, J., Wardell, D.A., Mikwa, J.-F., Kabuanga, J.M., Monga Ngonga, A.M., Oszwald, J. & Doumenge, C. (2019). Dynamique de la déforestation dans la Réserve de biosphère de Yangambi (République démocratique du Congo) : variabilité spatiale et temporelle au cours des 30 dernières années. *Bois et Forêts des Tropiques*, (341), 15-28.
- Landis, J.R. & Koch, G.G. (1977). The Measurement of Observer Agreement for Categorical Data, *Int. Biometric Soc.*, 33 (1), 159-174.
- Manguiengha, S.N., Mikolo-Yobo, C., Akpaca, I., Worah, J.A. & Nziengui, M. (2019). Contribution de la télédétection satellite et du SIG à la gestion durable des mangroves anthropisées de la forêt de la Mondah ; nord-ouest du Gabon. *International Journal of Engineering Science Invention (IJESI)*, 8 (10 Série II), 21-34.
- Mbaiyetom, H., Tientcheu, M.L.A., Ngankam, M.T., Taffo, J.B.W. & Tanougong, A.D. (2020). Dynamique spatio-temporelle de l'occupation du sol et du couvert végétal des parcs arborés du Département de la Nya, Sud du Tchad. *International Journal of Innovation and Applied Studies*, 31 (2), 370-379.
- Megevand, C., Mosnier, A., Hourticq, J., Klas, S., Nina, D., & Streck, C. (2013). *Dynamiques de déforestation dans le bassin du Congo: Réconcilier la croissance économique et la protection de la forêt*. Washington, DC, USA, Banque mondiale.
- Mirembe, O., 2005. *Echanges transnationaux, réseaux informels et développement local: une étude au Nord-Est de la République*

- Démocratique du Congo*. Thèse de doctorat en sciences sociales. Université Catholique de Louvain.
- Ndavaro K.N., Dramani R., Mulondi K. G., Muhindo Sahani W., Biaou S. S. H. & Natta K. A. (2021). Dynamique spatio-temporelle de l'occupation du sol et du couvert forestier dans les Hautes Terres Fraîches de Lubero (R.D. Congo). *Geo-Eco-Trop*, 45 (4), 641-658.
- Nsangua, B.M., Nshimba, H.N., Boyemba, F.B., Katusi, R.L., Mbayo, F.M. & Mbuyu, L.M. (2018). Etude de la variabilité structurale et floristique des forêts sur terre ferme en Chefferie de Bahema-Boga (Province De L'ituri, RDC). *European Scientific Journal*, 14 (30).
- Okanga-Guay, M., Ondo Assoumou, E., Akendengue Aken, I., Mpie Simba, C., Mombo, J-B., Obiang Ebanega, M., Mbadinga, M., Rogombe, L.G. & Mouketoutarazewicz, D. (2019). Suivi des changements spatiaux et environnementaux dans les mangroves de la province de l'Estuaire du Gabon. In Actes de la conférence scientifique internationale, 13–15 mars 2019, Hôtel Azalaï, Cotonou, Bénin.
- Oloukoi, J., Mama, V.J. & Agbo, F.B. (2006). Modélisation de la dynamique de l'occupation des terres dans le département des collines au Bénin. *Télédétection*, 6 (4), 305-323.
- Orekan, O.A.V., Plagbeto, H.A., Edea, E. & Sossou, M.D. (2019). Évolution actuelle des écosystèmes de mangrove dans le littoral béninois. In *Actes de la conférence scientifique internationale*, 13–15 mars 2019, Hôtel Azalaï, Cotonou, Bénin.
- Oswald, J., Arnauld De Sartre, X., Decaëns, T., Gond, V., Grimaldi, M., Lefebvre, A., De Araujo Fretas, R.L., Lindoso De Souza, S., Marichal, R., Veiga, I., Velasquez, E. & Lavelle, P. (2012). Utilisation de la télédétection et de données socio-économiques et écologiques pour comprendre l'impact des dynamiques de l'occupation des sols à Pacajà (Brésil). *Revue Française de Photogrammétrie et de Télédétection*, 198-199
- Oswald, J., Lefebvre, A., Arnauld De Sartre, X., Thales, M. & Valéry Gond, V. (2010). Analyse des directions de changement des états de surface végétaux pour renseigner la dynamique du front pionnier de Maçaranduba (Pará, Brésil) entre 1997 et 2006. Télédétection, Editions des Archives Contemporaines/Editions scientifiques GB/Gordon and Breach Scientific Publishers, 9 (2), 97-111.
- Ouattara, T.A., Kouame, K.F., Zo-Bi, I.C., Vaudry, R. & Grinand, C. (2021). Changements d'occupation et d'usage des terres entre 2016 et 2019 dans le Sud-Est de la Côte d'Ivoire : impact des cultures de rente sur la forêt. *Bois et Forêts des Tropiques*, (347), 89-104.
- Randriamalala, I.H. (2015). Analyse de la dynamique spatio-temporelle du Lac Alaotra et de l'occupation du sol dans le bassin versant du Maningory. Mémoire de fin d'études pour l'obtention du Diplôme d'Ingénieur en Sciences Agronomiques et Environnementales au grade de Master en Foresterie et Environnement, Université d'Antananarivo, 91 p
- Rifai, N., Khattabi, A., Moukrim, S., Arahou, M., & Rhazi (2018). Evaluation de la dynamique de l'occupation du sol dans la zone humide Ramsar de Tahaddart (Nord-Ouest du Maroc). *Revue d'Ecologie (Terre et Vie)*, 73 (2), 142-152.
- Samba, A.G., Kpoussa, F., Sabi Yo Boni, A., Houinsou, A. & Dossou Guedegbe, O. (2021). Cartographie De La Dynamique Spatio-Temporelle De L'occupation Des Terres Autour De La Reserve De Biosphère Transfrontalière Du W Dans La Commune De Banikoara Au Bénin (Afrique De L'ouest). *International Journal of Progressive Sciences and Technologies (IJPSAT)*, 24 (2), 185-196.
- Sangne, C.Y., Barima, Y.S.S., Bamba, I. & N'doume, C.-T.A. (2015). Dynamique forestière post-conflits armés de la Forêt classée du Haut-Sassandra (Côte d'Ivoire). *VertigO*, 15 (3).
- Soro, T. D., Kouakou, B. D., Kouassi, E. A., Soro, G., Kouassi, A. M., Kouadio, K. E., YEI, M.-S. O. & Soro, N. (2013). Hydroclimatologie et dynamique de l'occupation du sol du

- bassin versant du Haut Bandama à Tortiya (Nord de la Côte d'Ivoire). *VertigO*, 13 (3).
- Soulama, S., Kadeba, A., Nacoulma, B.M.I., Traore, S., Bachmann, Y. & Thiombiano, A. (2015). Impact des activités anthropiques sur la dynamique de la végétation de la réserve partielle de faune de Pama et de ses périphéries (sud-est du Burkina Faso) dans un contexte de variabilité climatique. *Journal of Applied Biosciences*, (87), 8047– 8064.
- Sylla, D., Ba, T., Diallo, M.D., Mbaye, T., Diallo, A., Peiry, J.L. & Guisse, A. (2015). Dynamique de l'occupation du sol de lacommune de Tèssékéré de 1984 à 2015 (FerloNord, Sénégal). *Journal of Animal & Plant Sciences*, 40 (3), 6674-6689.
- Tchatchou, B., Sonwa, D.J., Ifo, S & Iani, A.M. (2015). *Déforestation et dégradation des forêts dans le Bassin du Congo : Etat des lieux, causes actuelles et perspectives*. Papier occasionnel 120. Bogor, Indonésie: CIFOR.
- Toko Imorou, I., Arouna, O., Zakari, S., Djaouga, M., Thomas, O. & Kinmadon, G. (2019). Évaluation de la déforestation et de la dégradation des forêts dans les aires protégées et terroirs villageois du bassin cotonnier du Bénin. In Actes de la conférence scientifique internationale, 13–15 mars 2019, Hôtel Azalaï, Cotonou, Bénin.
- Tsewoue, M.R., Tchamba, M., Avana, M.L. & Tanougong, A.D. (2020). Dynamique spatio-temporelle de l'occupation du sol dans le Mounjo, Régiondu Littoral, Cameroun : influence sur l'expansion des systèmes agroforestiersà base de bananiers. *Int. J. Biol. Chem. Sci.* 14(2), 486-500.
- Useni Sikuzani, Y., Boisson, S., Cabala Kaleba, S., Nkuku Khonde, C., Malaisse, F., Halleux, J-F., Bogaert, J. & Kankumbi, F.M. (2020). Dynamique de l'occupation du sol autour des sites miniers le long du gradient urbain-rural de la ville de Lubumbashi, RD Congo. *Biotechnol. Agron. Soc. Environ*, 24(1), 14-27.
- Vyakuno, E. (2006). Pression anthropique et aménagement rationnel des hautes terres de Lubero en RDC. Rapports entre société et milieu physique dans une montagne équatoriale. Tomes I et II. Thèse de doctorat en Géographie, Université Toulouse 2-Le Mirail.